ORIGINAL PAPER



Atomic Force Microscopy of Transfer Film Development

Kathryn E. Shaffer¹ · Edward J. McCumiskey² · Brandon A. Krick³ · Jeffrey J. Ewin⁴ · Curtis R. Taylor² · Christopher P. Junk⁵ · Gregory S. Blackman⁶ · W. Gregory Sawyer⁷ · Angela A. Pitenis¹

Received: 11 April 2024 / Accepted: 9 July 2024 © The Author(s) 2024

Abstract

Atomic force microscopy (AFM) provides the opportunity to perform fundamental and mechanistic observations of complex, dynamic, and transient systems and ultimately link material microstructure and its evolution during tribological interactions. This investigation focuses on the evolution of a dynamic fluoropolymer tribofilm formed during sliding of polytetrafluoroethylene (PTFE) mixed with 5 wt% alpha-phase alumina particles against 304L stainless steel. Sliding was periodically interrupted for AFM topography scans. The average film roughness, the average friction coefficient, and polymer wear rate based on sample height recession were recorded as a function of increasing sliding cycles. Topographical maps suggested tribofilm nucleates in grooves of the steel countersample, spreads, and develops into a uniform film through sliding. Prominent nanoscale features were visible around 10,000 sliding cycles and thereafter. Scanning electron microscopy and energy-dispersive X-ray spectroscopy showed good correlations between these features and aluminum-rich domains, suggesting the presence of alumina particles on the surface.

Keywords Atomic force microscopy · Solid lubrication · Polytetrafluoroethylene · Alumina · Transfer film

1 Introduction

The fundamental mechanisms of friction and wear of solid lubricants are essential to designing longer-lasting materials and reducing waste. Polytetrafluoroethylene (PTFE) is a solid lubricant of particular importance to the tribology community due to its very low coefficient of friction and

- Angela A. Pitenis apitenis@ucsb.edu
- Materials Department, University of California, Santa Barbara, Santa Barbara, CA 93106, USA
- Department of Mechanical and Aerospace Engineering, University of Florida, Gainesville, FL 32611, USA
- Department of Mechanical Engineering, Florida A&M University-Florida State University College of Engineering, Tallahassee, FL 32310, USA
- ⁴ Naval Air Systems Command, Patuxent River, MD 20670, LICA
- ⁵ CJIdeas, LLC, Wilmington, DE, USA

Published online: 16 July 2024

- DuPont Electronics and Industrial, Wilmington, DE 19803, USA
- Department of BioEngineering, Moffitt Cancer Center, Tampa, FL 32611, USA

applicability in extreme environments (e.g., high thermal stability, resistance to chemical attack) [1–5]. However, PTFE suffers from low wear resistance, with wear rates approaching $k = 10^{-3} \text{ mm}^3/(\text{N} \cdot \text{m})$, rendering neat PTFE, an impractical choice for many engineering applications [6, 7]. To extend its utility, PTFE is filled with materials such as fibers, polymer blends, and nanoparticles [8–15]. In 2006, Burris and Sawyer discovered that the small addition of a specific alpha-phase alumina filler reduces the wear rate of PTFE by almost four orders of magnitude, to $k=1.3\times10^{-7}$ mm³/(N·m) [8]. The tribology community generally agrees that ultralow wear behavior is, in part, due to unique tribochemistry that occurs at these sliding interfaces and produces robust tribofilms on both the PTFE composite ("running film") and the metal countersurface ("transfer film") [16–22].

Wear resistance is also correlated with topographical changes in fluoropolymer-based transfer films [20, 23–27]. The formation of the transfer film occurs in three phases: (i) *run-in*, during which wear debris is generated and often swept aside, (ii) *transition*, during which small patches of transfer film adhere to the countersurface and accumulate, and (iii) *steady-state*, during which continuous transfer film formation occurs and wear rate decreases [26, 27]. The wear



rate of PTFE/alumina composites is dependent on the formation and maintenance of a robust transfer film [24].

The evolution of transfer film development has been extensively documented by optical imaging techniques [16, 17, 26–33]. Transfer film surface roughness (e.g., R_a) has been calculated from representative line scans sampled at various locations and often at the end of the sliding experiment using stylus or optical profilometry techniques [16, 28, 29]. Few studies have faithfully tracked the same location over time, and these were conducted using 2D techniques [33–36]. 3D techniques, such as AFM, have been leveraged in other tribological systems to study transfer films formed from liquid lubricants [37]. In this investigation, atomic force microscopy (AFM) was used to characterize the dynamically evolving 3D topography of the same region of a solid lubricant tribofilm from 0 to 1,000,000 reciprocating cycles (total sliding distance = 50.8 km). Our approach provides detailed insights into transfer film development at the microscale and may be used to correlate transfer film surface roughness with tribological performance.

2 Materials and Methods

2.1 Sample Preparation

Polytetrafluoroethylene (DuPont, Teflon® PTFE 7C resin, $\approx 30 \mu m$ particles) was weighed and hand-mixed with 5.0 wt.% alpha-phase alumina powder (Alfa Aesar, Stock $#44,652, \approx 60-80$ nm particles [25]). The PTFE/alumina powder mixture was dispersed in dry isopropanol using an ultrasonic horn (Branson Digital Sonicator 450 with a titanium tip), operating at approximately 40% amplitude (400 W) with 45 s rest in-between three 1-min sessions. The mixture dried for at least 1 week in a fume food to ensure all isopropanol evaporated. Roughly 13 g of dry powder mixture was compressed and free-sintered in an oven to 380°C for 4 h, then cooled to room temperature. Sintered polymer was machined into a $6.02 \times 6.35 \times 13.13$ mm rectangular prism for tribological testing. One of the 6.02×6.35 mm faces was polished with 800 grit silicon carbide sandpaper to an average surface roughness of Ra ≈ 150 nm. The polymer sample was sonicated in methanol for 30 min. and equilibrated in a fume hood for at least 3 h prior to testing.

The countersurface was composed of 304L stainless steel rectangular flat coupon ($38 \times 25 \times 3.7$ mm) with an average surface roughness of Ra ≈ 150 nm manufactured and lapped by Metal Samples Company (Alabama Specialty Products, Inc.). The metal countersample was cleaned by hand with mild detergent and water, then rinsed in acetone, followed by a rinse of isopropanol, and then sonicated for 30 min. in methanol and equilibrated in a fume hood for at least 3 h prior to testing.



A custom linear reciprocating tribometer, previously described in [10, 18, 20, 25, 27, 38] was used to conduct sliding experiments in a pin-on-flat configuration. The PTFE/alumina composite was mounted to a 6-channel force transducer (AMTI, MC3-6-1000), which measured normal and tangential (frictional) forces. The coefficients of friction calculated from these forces had an uncertainty less than $u(\mu) < 0.005$ [16]. A 61.2 mm bore Bimba pneumatic cylinder was used to load the composite against the countersurface to a nominal normal force of 250 N, resulting in an average contact pressure of approximately 6.54 MPa, which is less than 50% of the yield stress of PTFE [16]. The countersurface was mounted to a linear reciprocating ballscrew stage (Parker Hannifin, 406XR Stage) and slid against the stationary PTFE composite with a stroke of 25.4 mm at a velocity of 50.8 mm/s in ambient temperature (25°C) and relative humidity (30-50% RH).

Sliding experiments were interrupted periodically and the metal countersample was uninstalled from the tribometer for ex situ AFM measurements of the developing transfer film (Fig. 1). The tribometer and the AFM were housed on the same floor of the same building, and the sample was transported between the two instruments in a clean sample container with a lid, and the temperature and relative humidity was maintained for the duration of the study. Following AFM measurements, optical images of the metal countersurface were recorded using a D3X Nikon camera and a macro prime lens with 105 mm focal length. Following imaging, the countersample was reinstalled on the tribometer to within \pm 50 µm of the same location using a kinematic mount (Fig. 1). The polymer sample was not removed from the sample holder for any period of time until the end of the experiment (1,000,000 cycles) to mitigate positional uncertainties between the polymer sample and the countersurface and to reduce the risk of the transfer film re-developing following misalignment. Thus, wear rate of the polymer sample was calculated for each sliding interval based on the recession of height recorded by linear variable differential transformer (LVDT) sensor displacements (sampling frequency, f=1 kHz, RDP Group, DCTH200AG), as opposed to massbased measurements of wear rate. We re-arranged Archard's equation [39] to estimate the wear rate, k, as a function of sample height recession, h, nominal pressure, P, and sliding distance, d (Eq. 1):

$$k = \frac{h}{Pd} = \frac{h_f - h_i}{Pd} \tag{1}$$

Height recession, h, was calculated as the difference between the initial (h_i) and final position (h_f) of the LVDT



Tribology Letters (2024) 72:91 Page 3 of 9 91

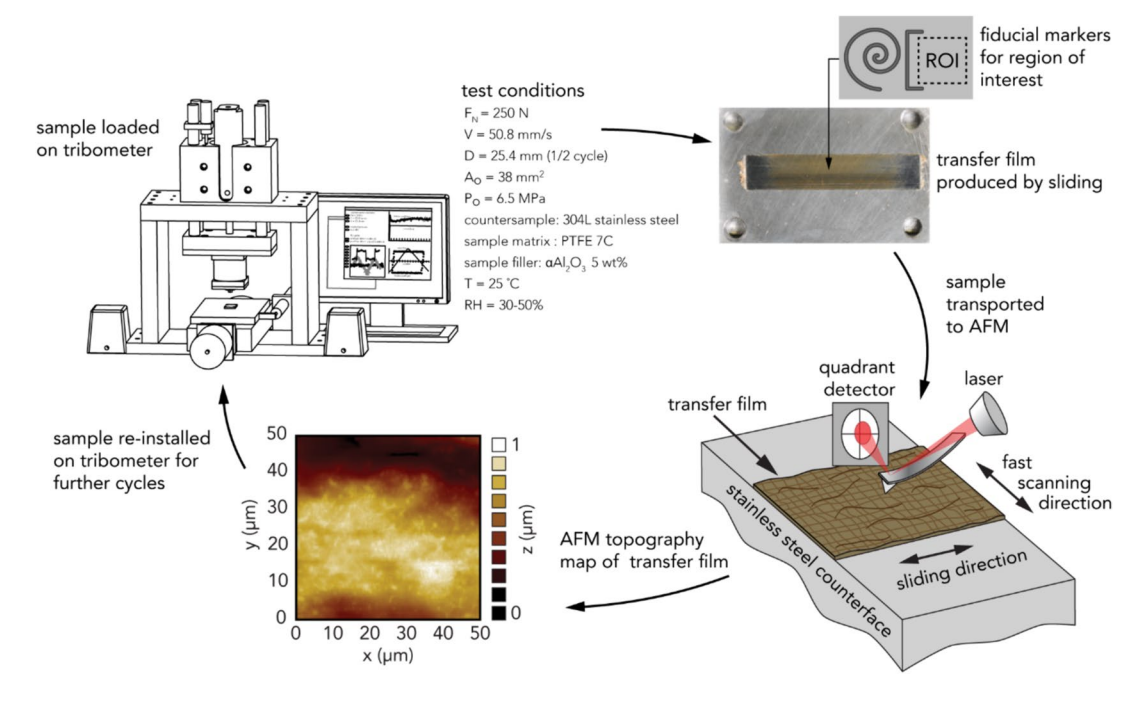


Fig. 1 Transfer films produced by sliding a polymer composite sample of PTFE 7C with 5 wt% alpha-phase alumina against a 304L stainless steel countersurface were investigated using AFM to observe topography evolution during periodic interruptions to sliding experiments

for each sliding interval. We emphasize that our LVDT-based wear measurements recorded material removal as well as elastic and plastic deformations, predominantly of the polymer composite. To reduce the uncertainty of height-based wear measurements, displacement was recorded by the LVDT only after the polymer sample had been loaded into contact with the countersurface to the nominal pressure for several minutes prior to sliding. Wear rates were calculated after the first sliding interval, which spanned 100 reciprocating cycles. We acknowledge that the Archard wear equation is conventionally used to evaluate steady-state conditions, where wear rate is assumed to vary linearly, after the run-in period. Wear rates are reported in units of mm³/(N·m).

2.3 Atomic Force Microscopy of Transfer Film Development

Tribofilm surface topography was characterized using atomic force microscopy (Asylum Research, MFP-3DTM AFM) in contact mode (0.5 Hz scan rate) with an ultrananocrystalline diamond AFM tip (NanoScience Instruments, NaDiaProbes ®, SKU: ND-CTIR1-4 S/N: 5390) with a manufacturer-specified radius of less than 50 nm. The scan size of each image was about $80 \times 80 \, \mu m$ and the scan angle was 90° for each scan. The AFM tip was periodically used to scan a smooth and clean silicon wafer to monitor tip damage or fouling. Prior to tribological testing, a diamond scribe and

a straight edge were used to manually mark a deep scratch into the metal countersurface (≈ 1 mm length) perpendicular to the direction of sliding, and a shallow scratch parallel to the sliding direction (≈ 5 mm length). An array of three fiducial rosettes ($\approx 500 \, \mu m$ diameter), each accompanied by an alignment marker ($\approx 100 \, \mu \text{m}$ wide bracket), were inscribed into the countersurface a few millimeters above the existing scratch using a three-sided diamond Berkovich indenter tip (axis-to-face angle of 65.3°) using the AFM software's lithography tool, following the methods in [40]. These fiducial markers were used to revisit the same three regions of interest for sequential AFM scans (Fig. 1). After tribological testing, each AFM height map was faithfully overlaid using SPIPTM—Scanning Probe Image Processor Software (Image Metrology), which resulted in near-continuous measurements of tribofilm development within 50×50 µm regions of interest. All AFM measurements were conducted within a soft-walled clean room (Clean Air Products) and were isolated from acoustic noise and vibrations.

2.4 Scanning Electron Microscopy

Scanning electron microscopy (ThermoFisher, Apreo C SEM) with energy-dispersive X-ray spectroscopy (EDAX, Octane Elect EDX detector) was used to map the elemental composition of transfer film asperities. To gain sufficient signal from EDX for accurate mapping, a high-voltage electron



91 Page 4 of 9 Tribology Letters (2024) 72:91

beam was needed. This voltage was significant enough to cause charge-induced damage to the insulating, fluoropolymer-rich tribofilm. Because of the damage that occurs when observing this material under SEM (Supplementary Fig. S1), an additional tribofilm was produced from a 'stripe test' (see Sect. 2.5 and Supplementary Sect. 2).

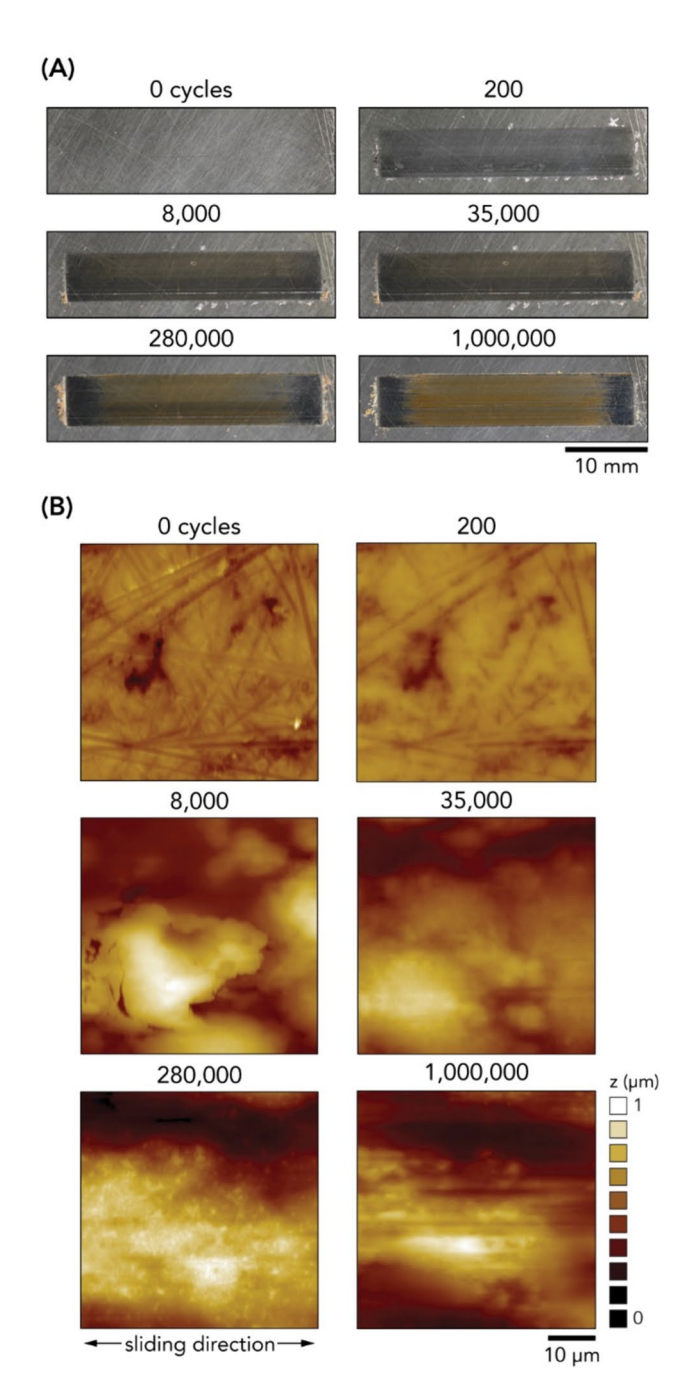


Fig. 2 Representative **A** optical images and **B** AFM topography maps of the 304L stainless steel countersurface depict transfer film evolution through sliding. Additional AFM images can be found in Dryad, an open-access data repository (see Data Availability Statement)



2.5 Stripe Test

In order to map asperities with EDX, an additional sample was created using a 'stripe test' [19, 20, 24, 29, 35, 41] whereby the stroke length decreased as the number of sliding cycles increased, exposing 12.7 mm sections of the transfer film developed from 10 k, 20 k, 30 k, 40 k, 50 k sliding cycles, and a 27.94 mm section of transfer film developed from 100 k sliding cycles (Supplementary Fig. S2). This sample was created using the methods described in Sects. 2.1 and 2.2 with the following exceptions: (i) the PTFE composite measured $6.32 \times 6.57 \times 16.83$ mm; (ii) the stainless steel countersurface measured 115 mm in length to accommodate the longer sliding distance required; (iii)

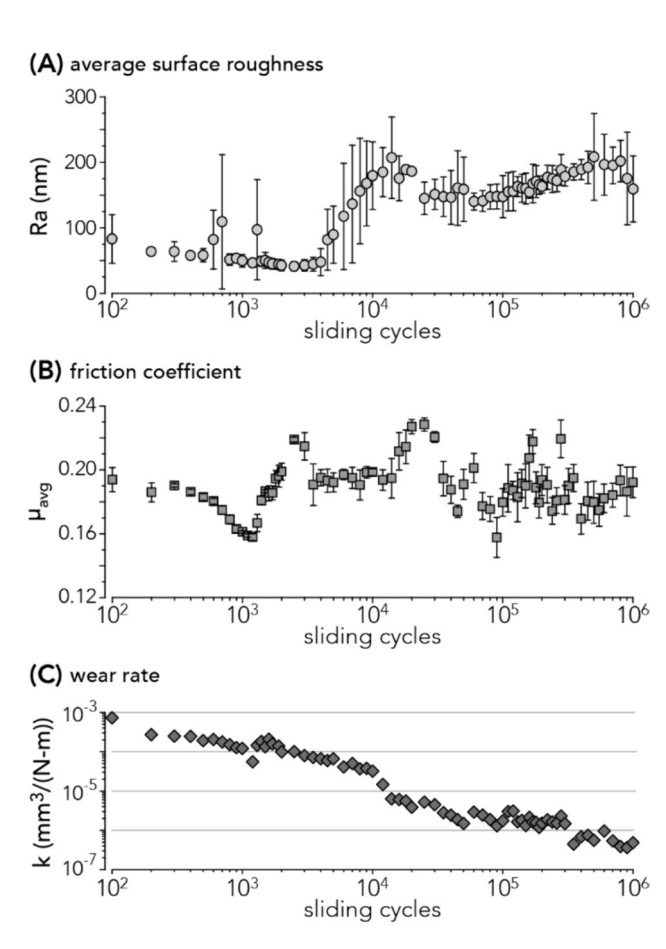


Fig. 3 A The average roughness, Ra, was calculated from AFM height maps using Igor Pro, the Asylum Research software package. Variability in average surface roughness across three regions of interest is represented by the error bars. B Average friction coefficients and C polymer composite wear rates were calculated from tribometer measurements at each periodic interruption to sliding experiments. Error bars represent the standard deviation in friction coefficient over each sliding interval [19]. Error bars indicating uncertainty in displacement-based wear rate measurements are smaller than the data points, in agreement with the previous mass-based wear rate uncertainty calculations [45]

Tribology Letters (2024) 72:91 Page 5 of 9 9

the countersurface remained mounted as interrupted AFM measurements were not required; (iv) the pin was removed at each stroke length change to calculate volume loss before being reinstalled on the tribometer (Supplementary Fig. S3).

2.6 Power Spectral Density Calculations

AFM height data for the original tribofilm experiment for the $50 \times 50 \,\mu m$ regions of interest were uploaded to the web application *contact.engineering* for power spectral density (PSD) calculations [42]. The PSD is the Fourier transform of the height autocorrelation function. The web application applied a PSD calculation to raw AFM height data to provide length-scale-dependent statistical information on surface roughness [43, 44]. A single-sided 1D PSD representation was calculated in the fast scan direction for the most accurate results, as recommended in [42]. Reliability of PSD calculations depended on the reliability of the AFM measurements. Therefore, any features unable to be detected accurately due to the AFM tip geometry (< 50 nm radius) or the resolution (points and lines) of the scan were not considered in the PSD calculation [42, 44].

3 Results and Discussion

3.1 Early Transfer Film Formation

Topographical measurements and optical images of the countersurface were periodically recorded as the tribofilm developed (Fig. 2). Supplementary Video 1 animates the evolution of surface topography with sliding cycles (also described in Supplementary Sect. 3). The stainless steel countersurface was recorded for reference to tribofilm

formation. Following a brief run-in period, the tribofilm entered the transition phase by 200 sliding cycles. During this phase, islands of PTFE composite were observed to nucleate and grow within the valleys of the countersurface. The filling of valleys corresponded to slight decreases in wear rate and average surface roughness across three regions (Fig. 3). The beginning of the steady-state phase occurred around 4000 cycles. From this point until about 10,000 cycles, patches of adhered transfer film grew, increasing surface roughness (from roughly 50 nm to 200 nm) while decreasing wear rate by about 5×.

Previous investigations of PTFE/alumina transfer films produced from stripe tests used X-ray photoelectron spectroscopy (XPS) to detect near-surface alumina [19]. In these studies, low concentrations of alumina within the top 10 nm of the transfer film were discovered within the first 100 cycles of sliding over a (3×3 mm) region of interest. However, in our investigation, AFM mapping (50×50 μ m) did not reveal any discernible topographical features resembling alumina deposits at this early stage of transfer film development. Previous investigations have reported that these alumina filler particles are friable and porous agglomerates of 1 μ m nanoparticles [25]. These particles may have fragmented from tribomechanical stresses into particle sizes much less than 50 nm, the diameter of the AFM tip, and thus the detection limit.

3.2 First Indication of Alumina by AFM

A transition from intermediate ($k \approx 5 \times 10^{-5} \text{ mm}^3/(\text{N} \cdot \text{m})$) to low wear ($k \approx 3 \times 10^{-6} \text{ mm}^3/(\text{N} \cdot \text{m})$) was observed between 10,000 and 20,000 cycles, corresponding to a plateau of the average roughness (Ra $\approx 175 \text{ nm}$) and bronze coloration in the transfer film. By visual inspection, AFM

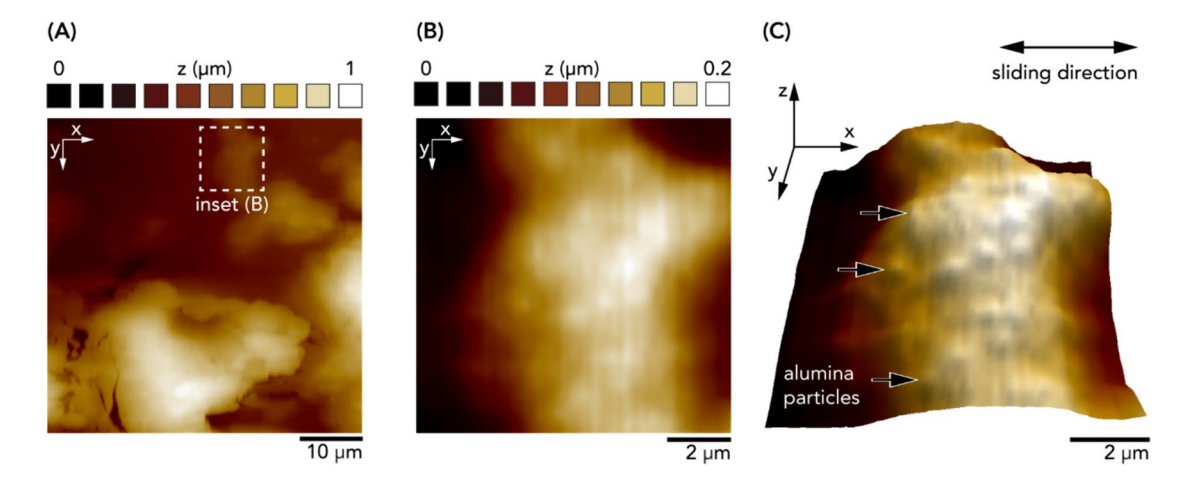


Fig. 4 A AFM topography map of transfer film developed at 8000 sliding cycles for the $50\times50~\mu m$ region of interest. **B** Inset of a $10\times10~\mu m$ region of interest. **C** 3D perspective of the $10\times10~\mu m$

region highlighting $< 1 \mu m$ features, likely alumina-rich deposits. Vertical streaks in (\mathbf{B}, \mathbf{C}) are artifacts of AFM tip rastering



91 Page 6 of 9 Tribology Letters (2024) 72:91

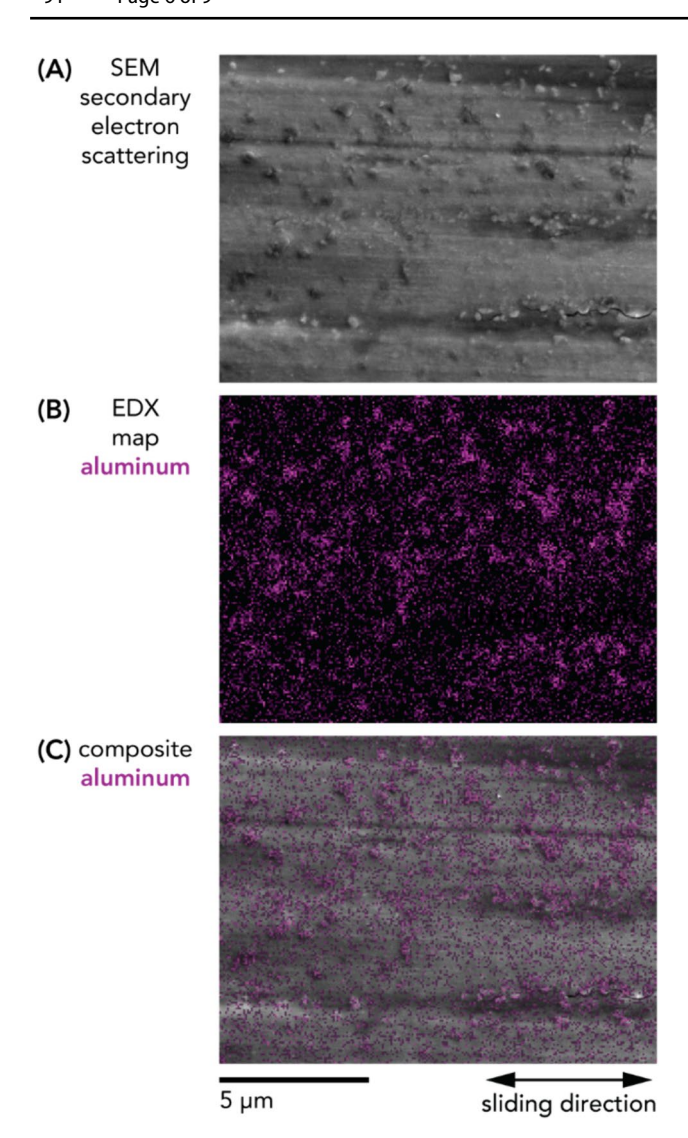


Fig. 5 A SEM secondary electron scattering micrograph of the stripe test transfer film at 50,000 sliding cycles. **B** EDX map of aluminum over the same region as the SEM micrograph. **C** Composite image overlaying the EDX map of aluminum on the SEM micrograph demonstrates raised asperities are aluminum rich and are likely alumina particles

topography revealed nanoparticle-like asperities around 10,000 sliding cycles (Fig. 4). Similar features were identified with AFM by 10,000 cycles on the stripe test sample (Supplementary Fig. S4, S5). EDX maps on the stripe test sample identified these asperities to be aluminum rich (Fig. 5), indicating the presence of alumina within these features. Following initial fluoropolymer deposition, smaller alumina fragments may agglomerate though tribomechanical mixing into sufficiently large particles above the detection limit of AFM.



3.3 Evolution of Transfer Film Topography

Power spectral density (PSD) calculations of AFM topography maps revealed variations in the PSD at different sliding cycles across wavevectors (Fig. 6A). Surface roughness at 0 cycles was dominated by grooves in the lapped stainless steel countersurface (Fig. 6B). The global drop in the PSD between 0 and 5000 cycles may be due to the transfer film filling in grooves in the countersurface, decreasing the roughness at all length scales (Fig. 6C). Similar observations have been recorded by others [28, 33, 38]. The subsequent increase in PSD at lower wavevectors (larger length scales) from 5000 to 100,000 sliding cycles could be attributed to the formation of larger rafts of fluoropolymer accumulating on the surface of the stainless steel (Fig. 6D, E). The increase in PSD at smaller length scales around 8,000 sliding cycles and onwards is hypothesized to be due to the emergence and accumulation of alumina particles (Fig. 6D, E). Illustrations of the probable surface topography at selected sliding cycles (Fig. 6B-E) are based on AFM topography maps.

3.4 Results of Tribological Measurements

Initial deposition of large and thin PTFE flakes effectively filled the deeper grooves of the countersurface and reduced friction coefficients from about $\mu \approx 0.20$ (cycle 100) to $\mu \approx 0.16$ (cycle 1,000). Following this initial drop, the average friction coefficient rose to $\mu \approx 0.20$ and then appeared insensitive to variations in the average surface roughness for the remainder of the sliding experiment (Fig. 3B). Our results suggest that macroscale, steady-state friction behavior may be independent of nanoscale or microscale topography of the tribofilm.

The polymer composite exhibited a steady decrease in wear rate with increasing sliding cycles from 100 to 1,000,000 cycles (Fig. 3C). The initial wear rate after 100 cycles closely matched the typical wear rate reported for unfilled PTFE, $k \approx 7 \times 10^{-4} \text{ mm}^3/(\text{N} \cdot \text{m})$ [23]. After just 1,000 cycles, the wear rate dropped nearly an order of magnitude to $k \approx 1 \times 10^{-4} \text{ mm}^3/(\text{N} \cdot \text{m})$. This drop in wear rate coincided with a local minimum in friction coefficient, $\mu \approx 0.16$. Between 10,000 and 20,000 cycles, the wear rate exhibited a precipitous decline from $k \approx 5 \times 10^{-5} \text{ mm}^3/(\text{N} \cdot \text{m})$ to $k \approx$ 3×10^{-6} mm³/(N·m). This stage in transfer film development was also marked by the emergence of near-surface alumina detected by AFM. Previous investigations have shown a gradual hardening of the tribofilms with increasing sliding cycles, which may be correlated to increased abundance of alumina and wear resistance [20, 27, 35]. In our investigation, the increased prevalence of nanoscale alumina features detected by AFM and the corresponding decrease in wear Tribology Letters (2024) 72:91 Page 7 of 9 91

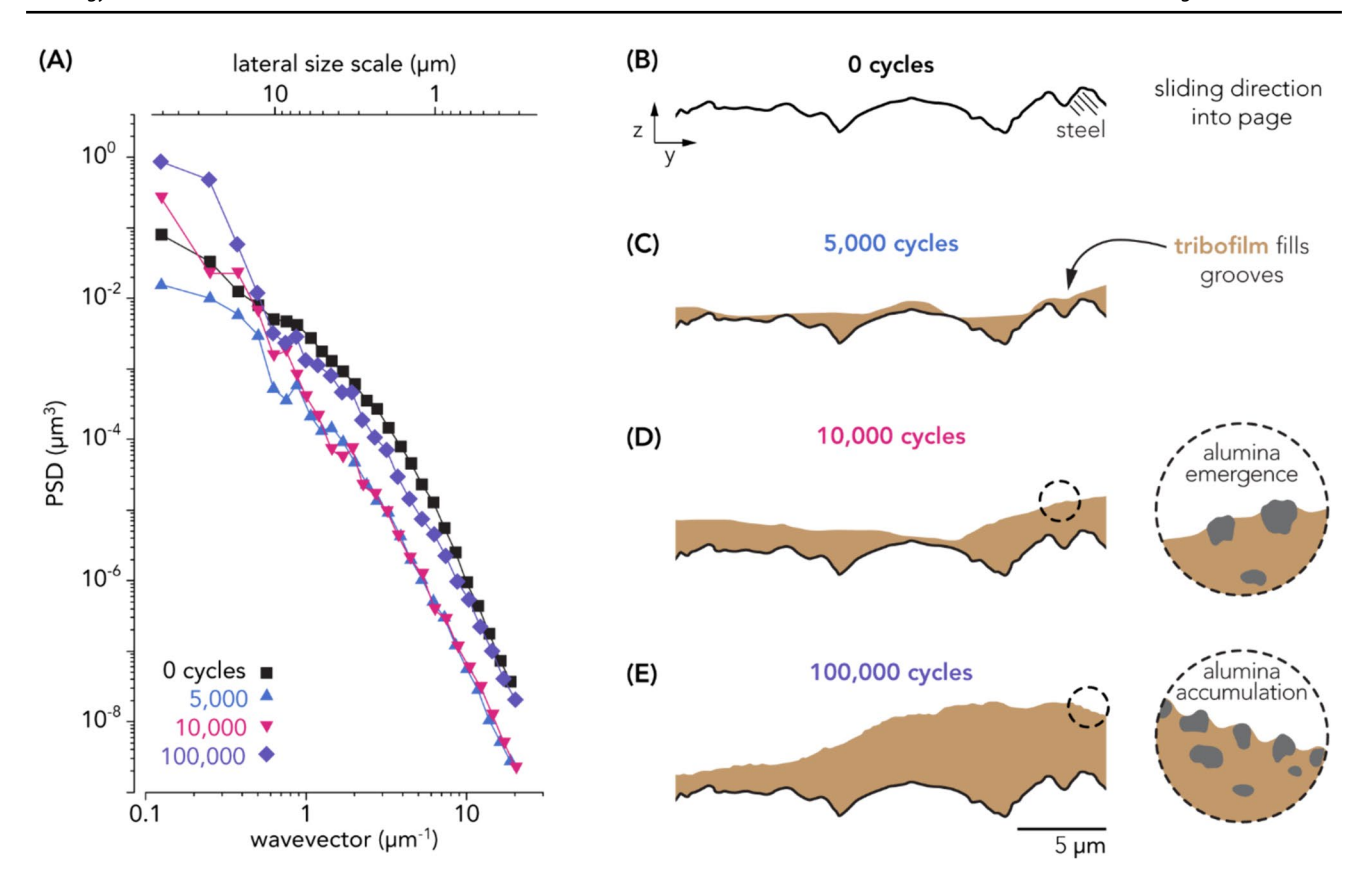


Fig. 6 A Power spectral density versus wavevector of AFM topography maps at sliding cycles: 0 (black squares), 5000 (blue up-triangles), 10,000 (magenta down-triangles), 100,000 (purple diamonds). **B–E** Illustrations of surface topography during transfer film devel-

opment. The scale bar is reasonable for the y-axis, but the z scale is exaggerated for illustrative purposes. Insets are illustrated with a 1:1 aspect ratio (Color figure online)

rate after 20,000 cycles ultimately led to a final wear rate at of $k \approx 5 \times 10^{-7}$ mm³/(N·m) at 1,000,000 cycles.

3.5 Limitations of the Present Study

Although this particular PTFE/alumina composite is known to achieve ultralow wear rates ($k < 1 \times 10^{-7}$ mm³/(N·m)), the ex situ approach in this study may have unintentionally accumulated microscale misalignments and resulted in a final wear rate roughly $5 \times$ higher than expected. The millimeter-scale fiducial markers manually inscribed into the metal countersurface parallel and perpendicular to the direction of sliding may have also impacted tribofilm formation and resulted in excess material removal [28, 33, 38]. The optical images in Fig. 2 depict a two-toned tribofilm above and below these fiducial markers; above, where AFM maps were collected, the tribofilm appears more robust. These optical images encapsulate the primary challenge associated with simultaneous contact-based approaches for surface topography and tribology.

This investigation was primarily based on evidence gathered from a probe-based technique. As such, errors may have

accumulated at small length scales ($<1 \, \mu m$) due to tip geometry. AFM tip raster artifacts appear at small length scales as shallow grooves due to contact mode (Fig. 4B, C). This could have contributed to similar small length scale PSD slopes across several sliding cycles (Fig. 6A).

The stripe test sample (Supplementary Fig. S3) exhibited somewhat higher wear rates than have been previously reported, which may have been due to the longer sliding path (initially 3.6×) than standard experiments. The longer sliding path necessitated more material transfer prior to the development of a robust transfer film and extended the runin and transition periods.

In this study, AFM height maps could not be stacked with respect to a stable reference (z=0). All AFM maps were scanned over a very small region within the center of the sliding path away from the edges of tribofilm development. For this reason, illustrations of the surface topography in Fig. 5 B-E are informed by AFM maps but do not include actual AFM data.



91 Page 8 of 9 Tribology Letters (2024) 72:91

4 Concluding Remarks

Atomic force microscopy was used to characterize transfer film development within a 50×50 µm region of interest formed through serial tribological interactions between PTFE/alumina composites and 304L stainless steel countersurfaces in ambient conditions. The friction coefficient was largely insensitive to microscale surface roughness after the first 1000 cycles. Nanoscale domains were detected around 10,000 cycles with AFM, confirmed to be aluminum rich with EDX, and are thought to contribute to improving wear performance. Topographical analysis of transfer film development reveals the complexities of dynamically mixing and evolving sliding interfaces.

Supplementary Information The online version contains supplementary material available at https://doi.org/10.1007/s11249-024-01893-x.

Acknowledgements The authors are grateful to Prof. Tevis Jacobs and Prof. Lars Pastewka for valuable discussions and to the members of the UC Santa Barbara Interfacial Engineering Laboratory for their support.

Author Contributions K.E.S. and A.A.P. wrote the main manuscript text. K.E.S., A.A.P., E.J.M., and B.A.K. prepared figures. All authors reviewed the manuscript.

Funding K.E.S. acknowledges support from the Department of Education Graduate Assistance in Areas of National Need (GAANN) Fellowship. A.A.P. acknowledges support from the NSF CAREER Award (CMMI-CAREER-2048043).

Data Availability The data supporting this manuscript are freely available at Dryad, an online data repository: https://doi.org/10.5061/dryad.zpc866thd.

Declarations

Conflict of interest The authors declare no conflict of interest.

Open Access This article is licensed under a Creative Commons Attribution 4.0 International License, which permits use, sharing, adaptation, distribution and reproduction in any medium or format, as long as you give appropriate credit to the original author(s) and the source, provide a link to the Creative Commons licence, and indicate if changes were made. The images or other third party material in this article are included in the article's Creative Commons licence, unless indicated otherwise in a credit line to the material. If material is not included in the article's Creative Commons licence and your intended use is not permitted by statutory regulation or exceeds the permitted use, you will need to obtain permission directly from the copyright holder. To view a copy of this licence, visit http://creativecommons.org/licenses/by/4.0/.

References

- Plunkett, R.J.: Tetrafluoroethylene polymers. US Patent 2230654A, 4 Feb 1941
- Renfrew, M.M., Lewis, E.E.: Polytetrafluoroethylene. Heat resistant, chemically inert plastic. Ind. Eng. Chem. 38, 870–877 (1946). https://doi.org/10.1021/ie50441a009

- Pooley, C.M., Tabor, D.: Friction and molecular structure: the behaviour of some thermoplastics. P. Roy. Soc. Lond. A Mat. 329, 251–274 (1972). https://doi.org/10.1098/rspa.1972.0112
- Biswas, S.K., Vijayan, K.: Friction and wear of PTFE—a review. Wear 158, 193–211 (1992). https://doi.org/10.1016/0043-1648(92)90039-B
- McKeen, L., Ebnesajjad, S.: Polytetrafluoroethylene: polymerization, properties, and microstructure. In: McKeen, L., Ebnesajjad, S. (eds.) Handbook of Thermoplastic Fluoropolymers, pp. 7–13. William Andrew Publishing, Norwich (2023)
- Blanchet, T.A., Kennedy, F.E.: Sliding wear mechanism of polytetrafluoroethylene (PTFE) and PTFE composites. Wear 153, 229–243 (1992). https://doi.org/10.1016/0043-1648(92)90271-9
- Tanaka, K., Uchiyama, Y., Toyooka, S.: The mechanism of wear of polytetrafluoroethylene. Wear 23, 153–172 (1973). https://doi. org/10.1016/0043-1648(73)90081-1
- Burris, D.L., Sawyer, W.G.: Improved wear resistance in alumina-PTFE nanocomposites with irregular shaped nanoparticles. Wear 260, 915–918 (2006). https://doi.org/10.1016/j.wear.2005.06.009
- Wang, Y., Yan, F.: Tribological properties of transfer films of PTFE-based composites. Wear 261, 1359–1366 (2006). https://doi.org/10.1016/j.wear.2006.03.050
- Jones, M.R., McGhee, E.O., Marshall, S.L., Hart, S.M., Urueña, J.M., Niemi, S.R., Pitenis, A.A., Schulze, K.D.: The role of microstructure in ultralow wear fluoropolymer composites. Tribol. T. 62, 135–143 (2019). https://doi.org/10.1080/10402004.2018. 1502855
- Sun, W., Liu, X., Liu, K., Wang, W., Ye, J.: Ultralow wear PTFE composites filled with beryllia and germania particles. Wear 450–451, 203270 (2020). https://doi.org/10.1016/j.wear.2020.203270
- Sun, W., Liu, X., Liu, K., Xu, J., Lu, Y., Ye, J.: Mechanochemical functionality of graphene additives in ultralow wear polytetrafluoroethylene composites. Carbon 184, 312–321 (2021). https:// doi.org/10.1016/j.carbon.2021.08.042
- Van Meter, K.E., Junk, C.P., Campbell, K.L., Babuska, T.F., Krick, B.A.: Ultralow wear self-mated PTFE composites. Macromolecules 55, 3924–3935 (2022). https://doi.org/10.1021/acs.macromol.1c02581
- Van Meter, K.E., Babuska, T.F., Junk, C.P., Campbell, K.L., Sidebottom, M.A., Grejtak, T., Kustas, A.B., Krick, B.A.: Ultralow wear behavior of iron–cobalt-filled PTFE composites. Tribol. Lett. 71, 4 (2022). https://doi.org/10.1007/s11249-022-01679-z
- Wei, J., Sun, W., Liu, K., Liu, X., Ye, J.: Tribochemical driven interfacial energy gradient in ultralow wear PTFE composite. Tribol. Int. 183, 108438 (2023). https://doi.org/10.1016/j.tribo int.2023.108438
- Krick, B.A., Ewin, J.J., Blackman, G.S., Junk, C.P., Sawyer, W.G.: Environmental dependence of ultra-low wear behavior of polytetrafluoroethylene (PTFE) and alumina composites suggests tribochemical mechanisms. Tribol. Int. 51, 42–46 (2012). https:// doi.org/10.1016/j.triboint.2012.02.015
- Krick, B.A., Hahn, D.W., Sawyer, W.G.: Plasmonic diagnostics for tribology: in situ observations using surface plasmon resonance in combination with surface-enhanced raman spectroscopy. Tribol. Lett. 49, 95–102 (2013). https://doi.org/10.1007/ s11249-012-0048-z
- Pitenis, A.A., Ewin, J.J., Harris, K.L., Sawyer, W.G., Krick, B.A.: In vacuo tribological behavior of polytetrafluoroethylene (PTFE) and alumina nanocomposites: the importance of water for ultralow wear. Tribol. Lett. 53, 189–197 (2014). https://doi.org/10.1007/ s11249-013-0256-1
- Pitenis, A.A., Harris, K.L., Junk, C.P., Blackman, G.S., Sawyer, W.G., Krick, B.A.: Ultralow wear PTFE and alumina composites: it is all about tribochemistry. Tribol. Lett. 57, 4 (2015). https://doi. org/10.1007/s11249-014-0445-6



Tribology Letters (2024) 72:91 Page 9 of 9 91

Harris, K.L., Pitenis, A.A., Sawyer, W.G., Krick, B.A., Blackman, G.S., Kasprzak, D.J., Junk, C.P.: PTFE tribology and the role of mechanochemistry in the development of protective surface films. Macromolecules 48, 3739–3745 (2015). https://doi.org/10.1021/acs.macromol.5b00452

- Alam, K.I., Bragaw, P., Burris, D.L.: Isolating the tribochemical and mechanical effects of nanofillers on PTFE wear. Wear 494–495, 204256 (2022). https://doi.org/10.1016/j.wear.2022. 204256
- Sun, W., Ye, J., Liu, X., Liu, K.: Atomistic insights into antiwear mechanisms and protective tribofilm formation in polytetrafluoroethylene composites. J. Tribol. T. ASME. 144, 091701 (2022). https://doi.org/10.1115/1.4053320
- Sawyer, W.G., Argibay, N., Burris, D.L., Krick, B.A.: Mechanistic studies in friction and wear of bulk materials. Ann. Rev. Mater. Res. 44, 395–427 (2014). https://doi.org/10.1146/annurev-matsci-070813-113533
- Urueña, J.M., Pitenis, A.A., Harris, K.L., Sawyer, W.G.: Evolution and wear of fluoropolymer transfer films. Tribol. Lett. 57, 9 (2015). https://doi.org/10.1007/s11249-014-0453-6
- Krick, B.A., Pitenis, A.A., Harris, K.L., Junk, C.P., Sawyer, W.G., Brown, S.C., Rosenfeld, H.D., Kasprzak, D.J., Johnson, R.S., Chan, C.D., Blackman, G.S.: Ultralow wear fluoropolymer composites: nanoscale functionality from microscale fillers. Tribol. Int. 95, 245–255 (2016). https://doi.org/10.1016/j.triboint.2015.10.002
- Ye, J., Khare, H.S., Burris, D.L.: Transfer film evolution and its role in promoting ultra-low wear of a PTFE nanocomposite. Wear 297, 1095–1102 (2013). https://doi.org/10.1016/j.wear.2012.12. 002
- Krick, B.A., Ewin, J.J., McCumiskey, E.J.: Tribofilm formation and run-in behavior in ultra-low-wearing polytetrafluoroethylene (PTFE) and alumina nanocomposites. Tribol. T. 57, 1058–1065 (2014). https://doi.org/10.1080/10402004.2014.933934
- Ye, J., Tao, B., Sun, W., Haidar, D.R., Alam, K.I., Liu, K., Burris, D.L.: The competing effects of counterface peaks and valleys on the wear and transfer of ultra-low wear alumina–PTFE. Tribol. Lett. 66, 12 (2017). https://doi.org/10.1007/s11249-017-0966-x
- Ye, J., Sun, W., Zhang, Y., Liu, X., Liu, K.: Measuring evolution of transfer film–substrate interface using low wear alumina PTFE. Tribol. Lett. 66, 100 (2018). https://doi.org/10.1007/ s11249-018-1054-6
- Alam, K.I., Dorazio, A., Burris, D.L.: Polymers tribology exposed: eliminating transfer film effects to clarify ultralow wear of PTFE. Tribol. Lett. 68, 67 (2020). https://doi.org/10.1007/ s11249-020-01306-9
- Alam, K.I., Burris, D.L.: Ultralow wear poly(tetrafluoroethylene): a virtuous cycle of wear reduction and tribochemical accumulation. J. Phys. Chem. C 125, 19417–19427 (2021). https://doi.org/ 10.1021/acs.jpcc.1c03885
- Alam, K.I., Garodia, A., Bragaw, P., Burris, D.L.: Independently tuning surface and subsurface reinforcement to optimize PTFE wear. Wear 510–511, 204516 (2022). https://doi.org/10.1016/j. wear.2022.204516
- Zhang, K., Liu, K., Gao, T., Qiao, Y., Zhang, Y., Liu, X., Wang, W., Ye, J.: The unrecognized importance of roughness

- directionality to polymer wear. Wear **486–487**, 204084 (2021). https://doi.org/10.1016/j.wear.2021.204084
- Sun, W., Liu, X., Song, Q., Liu, K., Wang, W., Lu, Y., Ye, J.: Mechanochemical effect of filler surface functionality on fluoropolymer tribology. Macromolecules 54, 6417–6429 (2021). https://doi.org/10.1021/acs.macromol.1c00395
- Sun, W., Song, Q., Liu, K., Liu, X., Ye, J.: The limit of adhesive debris retention: a case study using ultra-low wear Alumina– PTFE. Wear 496–497, 204274 (2022). https://doi.org/10.1016/j. wear.2022.204274
- Qi, Y., Sun, B., Wang, H., Zhang, Y., Gao, G., Zhang, P., Zheng, Y.: Quantitative measurement of morphological characteristics of PTFE composite transfer films based on computer graphics. Materials. 16, 1688 (2023). https://doi.org/10.3390/ma16041688
- Gosvami, N.N., Ma, J., Carpick, R.W.: An in situ method for simultaneous friction measurements and imaging of interfacial tribochemical film growth in lubricated contacts. Tribol. Lett. 66, 154 (2018). https://doi.org/10.1007/s11249-018-1112-0
- Harris, K.L., Curry, J.F., Pitenis, A.A., Rowe, K.G., Sidebottom, M.A., Sawyer, W.G., Krick, B.A.: Wear debris mobility, aligned surface roughness, and the low wear behavior of filled polytetrafluoroethylene. Tribol. Lett. 60, 2 (2015). https://doi.org/10.1007/ s11249-015-0581-7
- Archard, J.F.: Contact and rubbing of flat surfaces. J. Appl. Phys. 24, 981–988 (1953). https://doi.org/10.1063/1.1721448
- McCumiskey, E.J., Rudawski, N.G., Sawyer, W.G., Taylor, C.R.: Three-dimensional visualization of nanoscale structure and deformation. J. Mater. Res. 28, 2637–2643 (2013). https://doi.org/10.1557/jmr.2013.245
- Wahl, K.J., Singer, I.L.: Role of the third body in life enhancement of MoS₂. In: Dowson, D., Taylor, C.M., Childs, T.H.C., Dalmaz, G., Berthier, Y., Flamand, L., Georges, J.-M., Lubrecht, A.A. (eds.) Tribology S, pp. 407–413. Elsevier (1996)
- Röttger, M.C., Sanner, A., Thimons, L.A., Junge, T., Gujrati, A., Monti, J.M., Nöhring, W.G., Jacobs, T.D., Pastewka, L.: Contact. engineering—Create, analyze and publish digital surface twins from topography measurements across many scales. Surf. Topogr. Metrol. Prop. 10(3), 035032 (2022)
- Jacobs, T.D.B., Junge, T., Pastewka, L.: Quantitative characterization of surface topography using spectral analysis. Surf. Topogr. Metrol. Prop. 5, 013001 (2017). https://doi.org/10.1088/2051-672X/aa51f8
- Sanner, A., Nöhring, W.G., Thimons, L.A., Jacobs, T.D.B., Pastewka, L.: Scale-dependent roughness parameters for topography analysis. Appl. Surf. Sci. 7, 100190 (2022). https://doi.org/10.1016/j.apsadv.2021.100190
- Schmitz, T.L., Action, J.E., Burris, D.L., Ziegert, J.C., Sawyer, W.G.: Wear-rate uncertainty analysis. J. Tribol.—T. ASME. 126, 802–808 (2004). https://doi.org/10.1115/1.1792675

Publisher's Note Springer Nature remains neutral with regard to jurisdictional claims in published maps and institutional affiliations.

